Seismic Protection of Structures with Supplemental Rotational Inertia

Nicos Makris, Ph.D.* and Georgios Kampas, Ph.D.

Department of Civil, Environmental and Construction Engineering, University of Central Florida, Orlando, FL 32816

**Corresponding Author. Email of Corresponding author: Nicos.Makris@ucf.edu*

ABSTRACT

In this paper we investigate the alternative strategy of suppressing ground-induced vibrations with supplemental rotational inertia. The proposed concept employs a rack-pinion-flywheel system that its resisting force is proportional to the relative acceleration between the vibrating mass and the support of the flywheels. This arrangement, known in the mechanical networks literature as the "inerter", complements the traditional supplemental damping and stiffness strategies used for the seismic protection of structures. The paper shows that the seismic protection of structures with supplemental rotational inertia has some unique advantages; in particular in suppressing the spectral displacements of long period structures –a function that is not efficiently achieved with large values of supplemental damping. The paper shows that this happens at the expense of transferring appreciable forces at the support of the flywheels and proceeds by examining to what extent the finite stiffness and damping of the support of the flywheels affects the dynamics of the system. The proposed concept may be attractive for the seismic protection of bridges given that the rack-pinion-flywheel system strategy can accommodate large displacements.

INTRODUCTION

Most common civil engineering structures are framing systems or shear-beam type structures which when subjected to lateral inertial loading the dominant motion of their masses (floors in buildings or bridge decks) is a linear translation. In such structural systems the seismic induced displacements are primarily controlled with elasticity, damping and strength (Clough and Penzien 1975; Kelly 1997; Constantinou et al. 1998; Naeim and Kelly 1999; Chopra 2000; Makris and Chang 2000a, 2000b; Black et al. 2004; Symans et al. 2008). A notable exception to this kind of response is the seismic response of the free-standing slender column, which upon uplifting it enters rocking motion (Kirkpatrick 1927; Housner 1963). It is because of this rotational motion that most of the seismic resistance of the free-standing rocking column originates from the difficulty to mobilize its rotational inertia (Makris 2014a, 2014b, Makris and Kampas 2016 and references reported therein) –a quantity that is proportional to the square of the column size.

The main motivation of this paper is to examine whether the unique advantages for seismic protection that result from the mobilization of rotational inertia can be implemented in traditional framing systems where the dominant motion of their masses is translation (no rotations). The paper proposes the use of supplemental flywheels which are engaged in motion through a rack-and-pinion system (Patton 1980; PTDA 2014; among others). The proposed concepts may also apply to the seismic protection of bridges given the more-than-a-century-long experience of power transmission technology in movable bridges (Engineering News 1913; Hahin 1998; Movable Bridge Engineering 2014; among others). The advantage of a set of flywheels which are engaged in motion through a rack-and-pinion system is that the supplemental inertia is proportional only to the relative acceleration between the structure and the support of the flywheels. This mechanical arrangement that is coined “the inerter” has been proposed in the context of synthesis of mechanical networks in an effort to achieve a completely analogous correspondence between mechanical and electrical circuits (Smith 2002; Papageorgiou and Smith 2005). More recently the concept of a two-terminal device, that its output force is proportional to the relative acceleration has been proposed to enhance the performance of tuned mass dampers (Marian and Giaralis 2013, 2014; Giaralis and Taflanidis 2015). Furthermore, the proposed rack-pinion-flywheel can accommodate large, translational displacements which may challenge the implementation of other seismic protection devices such as fluid or metallic dampers.

REDUCTION OF VIBRATIONS WITH SUPPLEMENTAL ROTATIONAL INERTIA

Figure 1(left) depicts a single-degree-of-freedom structure with stiffness k and mass, m. A stiff shevron frame supports a flywheel with radius, R_1 and mass m_{W1} which can rotate about an axis O. First we consider the case of a very stiff chevron frame that its deformation is negligible to the translational displacement, $u(t)$, of the SDOF structure. Concentric to the flywheel there is an attached pinion with radius, ρ_1, engaged to a linear rack connected to

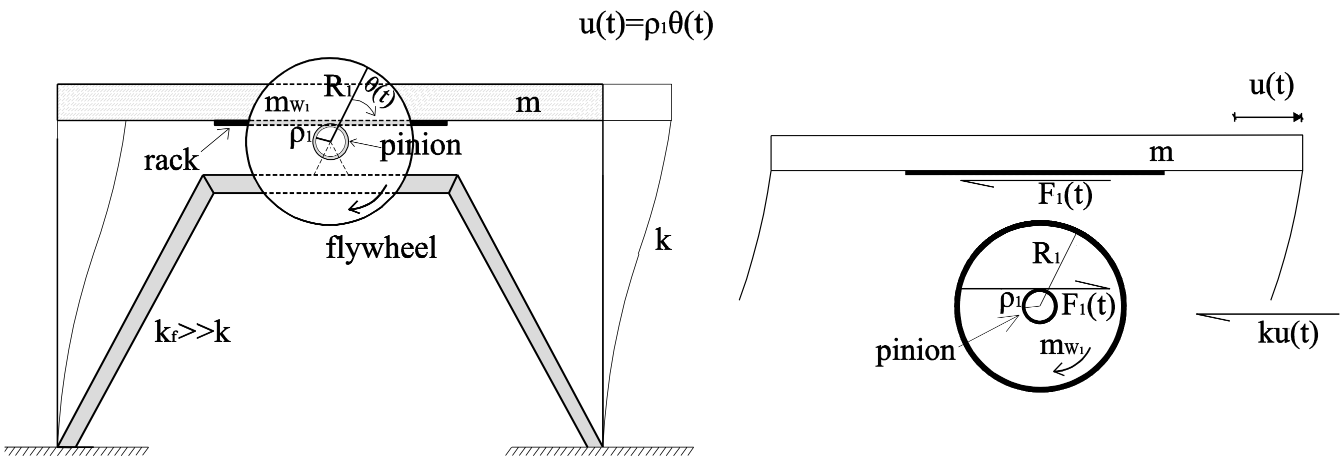

Fig. 1. Left: A single-degree-of-freedom structure with mass, m, and stiffness, k, with supplemental rotational inertia from a flywheel with radius, R, supported on a chevron frame with stiffness, k_f, that is much larger than k; Right: Free-body diagram of the vibrating mass, m, when engaged to the pinion of the flywheel shown below.

the bottom of the vibrating mass, m, of the SDOF. With this arrangement when the mass m undergoes a positive displacement, $u(t)$, the flywheel is subjected to a clockwise rotation, $\theta_1(t)$. Given that there is no slipping between the rack and the pinion,

$$\theta_1(t) = \frac{u(t)}{\rho_1} \tag{1}$$

Figure 1(right) shows the free-body diagrams of the vibrating mass, m, and the rotating pinion-flywheel system. For a positive displacement, $u(t)$, to the right, the internal force, F_1, at the rack-pinion interface opposes the motion (to the left). Accordingly, dynamic equilibrium of the vibrating mass when subjected to a ground acceleration, $\ddot{u}_g(t)$, gives

$$m[\ddot{u}(t) + \ddot{u}_g(t)] = -ku(t) - F_1(t) \tag{2}$$

where the internal force $F_1(t)$ needs to satisfy the moment equilibrium of the flywheel about point O

$$I_{W1}\ddot{\theta}_1(t) = F_1(t)\rho_1 \tag{3}$$

In equation (3), $I_{W1} = (1/2)m_{W1}R_1^{\,2}$, is the moment of inertia of the flywheel about point O. Substitution of equation (3) into (2) in association with equation (1) gives

$$(1+\frac{1}{2}\frac{m_{W1}}{m}\frac{R_1^{\,2}}{\rho_1^{\,2}})\ddot{u}(t)+\omega_o^{\,2}u(t)=-\ddot{u}_g(t) \tag{4}$$

where, $\omega_0=\sqrt{k/m}$, is the natural frequency of the structure when the pinion-flywheel is disengaged. Upon dividing with the acceleration coefficient, equation (4) gives,

$$\ddot{u}(t)+\underbrace{\frac{\omega_o^{\,2}}{1+\frac{1}{2}\frac{m_{W1}}{m}\frac{R_1^{\,2}}{\rho_1^{\,2}}}}_{\textit{Lengthening of the period}}u(t)=-\underbrace{\frac{1}{1+\frac{1}{2}\frac{m_{W1}}{m}\frac{R_1^{\,2}}{\rho_1^{\,2}}}}_{\substack{\textit{Suppression of the input}\\ \textit{ground motion}}}\ddot{u}_g(t) \tag{5}$$

Equation (5) indicates that the engagement of the flywheel in a rotational motion lengthens the vibration period of the structure and most importantly it suppresses the level of ground shaking given that the denominator in the right hand side is always larger than unity.

AMPLIFICATION OF THE ROTATIONAL INERTIA EFFECT

Equation (5) dictates that when the SDOF with stiffness, k, and mass, m, is equipped with a single flywheel with radius, R_1, and mass, m_{W1}, together with a pinion with radius, ρ_1, the input ground acceleration is divided by the term

$$1+\sigma=1+\frac{1}{2}\frac{m_{W1}}{m}\frac{R_1^{\,2}}{\rho_1^{\,2}} \tag{6}$$

While the denominator $=1+\sigma$ is always larger than unity and the radius of the flywheel, R_1, may be as large as ten (10) times the radius of the pinion, ρ_1, (or even larger, $\frac{R_1^{\,2}}{\rho_1^{\,2}}>100$), the suppression coefficient $=\frac{1}{2}\frac{m_W}{m}\frac{R_1^{\,2}}{\rho_1^{\,2}}$ may remain small given that the mass of the flywheel, m_{W1}, is appreciably smaller than the mass of the structure, m. Nevertheless, the effect of supplementing framing structures with rotational inertial may be amplified by installing two (or more) flywheels in series where the first flywheel is a gear-wheel as shown in Figure 2.

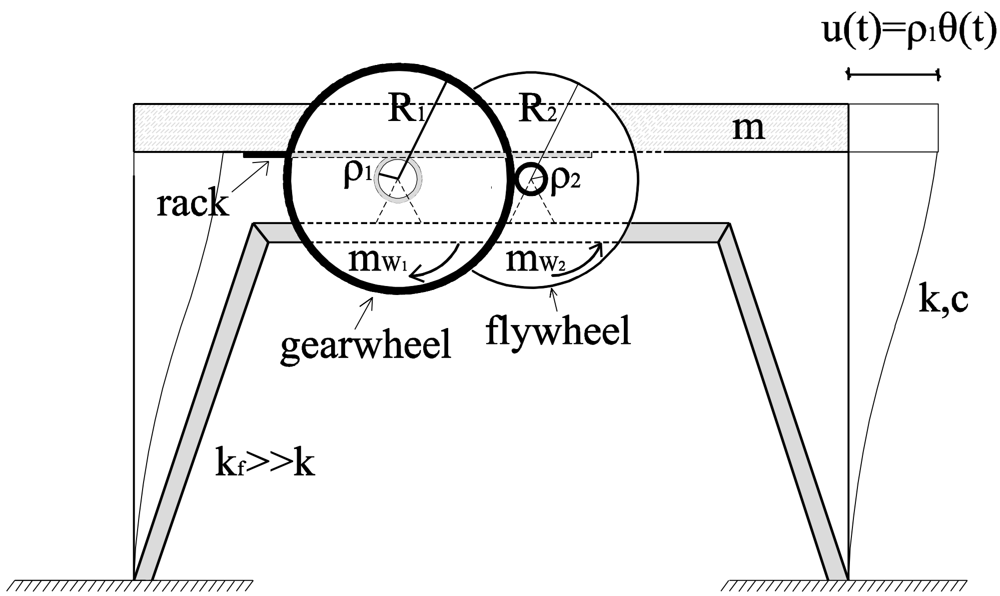

Fig. 2. More than one flywheels in series that amplify the effect of supplemental rotational inertia.

For the dynamic analysis of a system shown in Fig. 2 one can certainly proceed with a direct formulation as was done in the previous section for a single flywheel. Nevertheless, given that this proposed concept may involve several flywheels we proceed with a variational formulation where there is no need to calculate the internal forces, F_{j+1}, between the flywheel j and the pinion of the flywheel, $j+1$. Application of Lagrange's equation to the system shown in Fig. 4 gives

$$\frac{d}{dt}\left(\frac{\partial \mathcal{L}}{\partial \dot{u}}\right)-\frac{\partial \mathcal{L}}{\partial u}=-\frac{dW}{du} \tag{7}$$

where, $\mathcal{L}=T\text{-}V$, is the Langrangian function (difference between the kinetic energy, T, and the potential energy, V, of the system) and W is the work done by the external field forces. During an admissible translation δu, the variation of the work, $\delta W = m\ddot{u}_g(t)\delta u$ and given that $\delta W = \frac{dW}{du}\delta u$, one obtains

$$\frac{dW}{du}=m\ddot{u}_g(t) \tag{8}$$

For the two-wheel SDOF system shown in Figure 2, the kinetic energy is

$$T = \frac{1}{2} m\dot{u}^2(t) + \frac{1}{2} I_{W1}\dot{\theta}_1^{\,2}(t) + \frac{1}{2} I_{W2}\dot{\theta}_2^{\,2}(t) \tag{9}$$

where $\theta_1(t)$ is given by equation (1) and $\theta_2(t)$ satisfies compatibility of the displacements between the gearwheel and the pinion of the second flywheel.

$$\theta_2(t) = \theta_1(t)\frac{R_1}{\rho_2} \tag{10}$$

Substitution of equations (1) and (10) into equation (9), together with that $I_{W1} = \frac{1}{2} m_{W1} R_1^{\,2}$ and $I_{W2} = \frac{1}{2} m_{W2} R_2^{\,2}$, gives the expression of the kinetic energy only in terms of the velocity of the SDOF.

$$T = \frac{1}{2} m\dot{u}^2(t)\left(1 + \frac{1}{2}\frac{m_{W1}}{m}\frac{R_1^{\,2}}{\rho_1^{\,2}} + \frac{1}{2}\frac{m_{W2}}{m}\frac{R_1^{\,2} R_2^{\,2}}{\rho_1^{\,2}\rho_2^{\,2}}\right) \tag{11}$$

The potential energy of the SDOF is merely,

$$V = \frac{1}{2} k u^2(t) \tag{12}$$

and the Lagrangian function of the SDOF shown in Figure 2 assumes the expression:

$$\mathcal{L} = \frac{1}{2} m\dot{u}^2(t)\left(1 + \frac{1}{2}\frac{m_{W1}}{m}\frac{R_1^{\,2}}{\rho_1^{\,2}} + \frac{1}{2}\frac{m_{W2}}{m}\frac{R_1^{\,2} R_2^{\,2}}{\rho_1^{\,2}\rho_2^{\,2}}\right) - \frac{1}{2} k u^2(t) \tag{13}$$

Substitution of equations (13) and (8) into Lagrange equation (7) gives the equation of motion of the SDOF structure with a two flywheel rotational inertia system as shown in Figure 2.

$$\left(1 + \frac{1}{2}\frac{m_{W1}}{m}\frac{R_1^{\,2}}{\rho_1^{\,2}} + \frac{1}{2}\frac{m_{W2}}{m}\frac{R_1^{\,2} R_2^{\,2}}{\rho_1^{\,2}\rho_2^{\,2}}\right)\ddot{u}(t) + \omega_0^{\,2} u(t) = -\ddot{u}_g(t) \tag{14}$$

where, $\omega_0 = \sqrt{k/m}$, is again the natural frequency of the SDOF structure when is disengaged from the flywheel system. Accordingly, the equation of motion of the SDOF structure assumes the form

$$\ddot{u}(t) + \frac{\omega_0^{\,2}}{1+\sigma} u(t) = -\frac{1}{1+\sigma} \ddot{u}_g(t) \tag{15}$$

where for the case of a two-flywheel rotational inertia system, the suppression coefficient, σ, is

$$\sigma = \frac{1}{2}\frac{m_{W1}}{m}\frac{R_1^{\,2}}{\rho_1^{\,2}} + \frac{1}{2}\frac{m_{W2}}{m}\frac{R_1^{\,2}R_2^{\,2}}{\rho_1^{\,2}\rho_2^{\,2}} \tag{16}$$

For a ratio $R_2/\rho_2 \approx 10$, the second term in equation (16) is two orders of magnitude larger than the first term. When n flywheels are installed in series, the rotation of the nth flywheel is

$$\theta_n = \theta_1 \frac{R_1}{\rho_2}\frac{R_2}{\rho_3}\dots\frac{R_{n-1}}{\rho_n} = \theta_1 \prod_{j=2}^{n} \frac{R_{j-1}}{\rho_j} \tag{17}$$

By virtue of equation (17), the kinetic energy of the nth flywheel is

$$T_n = \frac{1}{2} I_{Wn}\theta_n^{\,2}(t) = \frac{1}{2}\frac{m_W}{2} R_n^{\,2}\theta_1^{\,2} \prod_{j=2}^{n}\left(\frac{R_{j-1}}{\rho_j}\right)^2 ; \tag{18}$$

and upon replacing, $\theta_1(t)$ with $u(t)/\rho_1$, equation (18) gives

$$T_n = \frac{1}{2}\frac{m_W}{2}\frac{R_1^{\,2}R_2^{\,2}\dots R_n^{\,2}}{\rho_1^{\,2}\rho_2^{\,2}\dots\rho_n^{\,2}}\dot{u}^2(t) \tag{19}$$

Consequently, the equation of motion of the SDOF structure equipped with a n-flywheel rotational inertia system is given again by equation (15); where now the suppression coefficient, σ, is given by

$$\sigma = \frac{1}{2}\frac{m_{W1}}{m}\frac{R_1^{\,2}}{\rho_1^{\,2}} + \frac{1}{2}\frac{m_{W2}}{m}\frac{R_1^{\,2}R_2^{\,2}}{\rho_1^{\,2}\rho_2^{\,2}} + \dots + \frac{1}{2}\frac{m_{Wn}}{m}\frac{R_1^{\,2}R_2^{\,2}\dots R_n^{\,2}}{\rho_1^{\,2}\rho_2^{\,2}\dots\rho_n^{\,2}} \tag{20}$$

For a ratio $R_j / \rho_j \approx 10$, each term in equation (20) is two order of magnitude larger than the previous term, therefore for any number, n , of flywheels selected, the suppression coefficient is merely governed by the last term of equation (20).

$$\sigma \approx \frac{1}{2}\frac{m_{Wn}}{m}\frac{R_1{}^2 R_2{}^2 ... R_n{}^2}{\rho_1{}^2 \rho_2{}^2 ... \rho_n{}^2} \tag{21}$$

Accordingly, regardless how small is the ratio m_{Wn} / m , the suppression coefficient σ can assume any desired value with the sufficient size and number of flywheels. Figure 3 (left) shows a schematic of the mass-spring-inerter system described by equation (15). It is a linear system that does not dissipate any energy–the vibration suppression happens by transferring kinetic energy from the vibrating mass to the rotating flywheel.

FORCE TRANSFERRED TO THE CHEVRON FRAME

The force transferred to the chevron frame, F_1, is an internal force, which can be recovered from the final form of the equation of motion given by (15) in association with the original dynamic equilibrium equation (2) of the vibrating mass that is expressed as

$$m\ddot{u}(t) + F_1(t) + ku(t) = -m\ddot{u}_g(t) \tag{22}$$

Equation (15) is expressed as

$$m\ddot{u}(t) + \sigma m\ddot{u}(t) + ku(t) = -m\ddot{u}_g(t) \tag{23}$$

Upon subtracting equation (23) from (22) one obtains the internal force transferred to a stiff chevron frame

$$F_1(t) = \sigma m\ddot{u}(t) = M_R\ddot{u}(t) \tag{24}$$

where σ is the suppression coefficient given by equation (20) or (21). The quantity $M_R = \sigma m$ is an additional apparent mass in the system (namely the rotational mass $= M_R$) which is due to the rotational inertia of the flywheels, Equation (24) offers the force transferred to a stiff chevron frame that its deformation is negligible compared to the

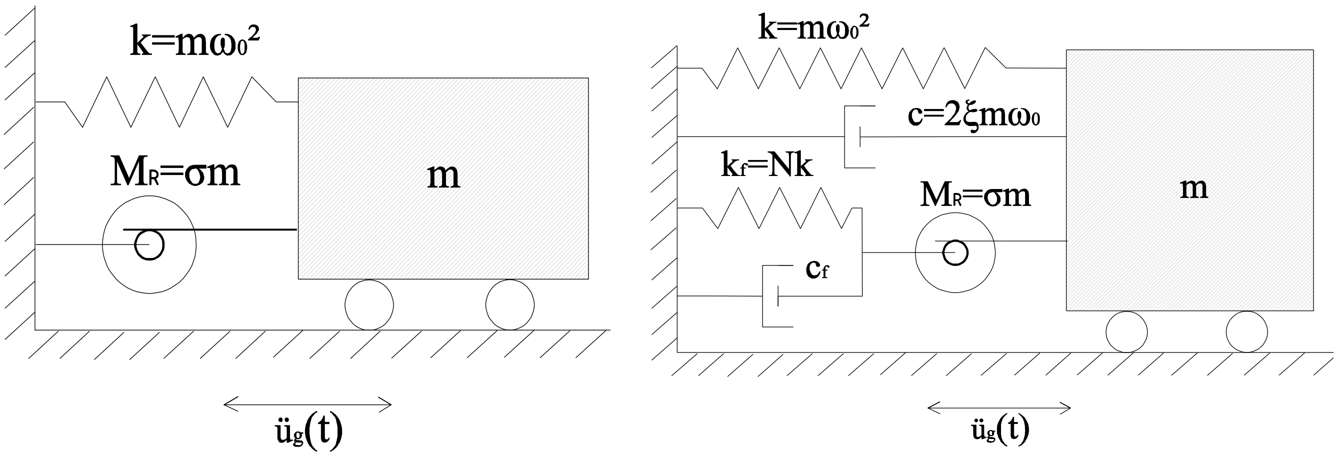

Fig. 3. Left: Schematic of a mass-spring-inerter single-degree-of-freedom system: the inerto-elastic oscillator; Right: The inerto-visco-elastic oscillator.

displacement of the structure, $u(t)$, and it indicates that in this case, $F_1(t)$, is proportional to the relative acceleration of the SDOF- system. The case of a "flexible" chevron frame is treated in a following section.

THE NEED FOR TWO PARALLEL INERTIA SYSTEMS AND THE OPPORTUNITY FOR ENERGY HARVESTING

In the previous sections we introduced the concept of supplemental rotational inertia for the seismic protection of traditional framing systems and it was shown that the proposed concept is physically realizable with the arrangement of more than one flywheel in series so that the amplification coefficient given by equation (20) becomes sufficiently large.

In the ideal case where energy is not dissipated through friction or other energy dissipation mechanism, equation (15) describes an undamped system (see Figure 3-left) in which part of the ground induced energy is transferred in to the flywheels. Figure 4 (left) plots the relative displacement, velocity, force transferred to the chevron frame and absolute acceleration of the inerto-elastic oscillator show in Figure 3 (left) with $T_0 = 1.0s$ when subjected to a one-sine acceleration with acceleration amplitude $a_p = 0.5g$ and pulse duration $T_p = 0.5s$. The shaded stripes in Figure 4 correspond to the segments where the magnitude of the relative velocity of the oscillator described by equation (15) reduces on its way to reach a peak displacement. During this interval, the flywheels have built angular momentum and now as the translating mass tends to move slower the flywheels may drive the mass; therefore, inducing deformations – a situation that is not desirable.

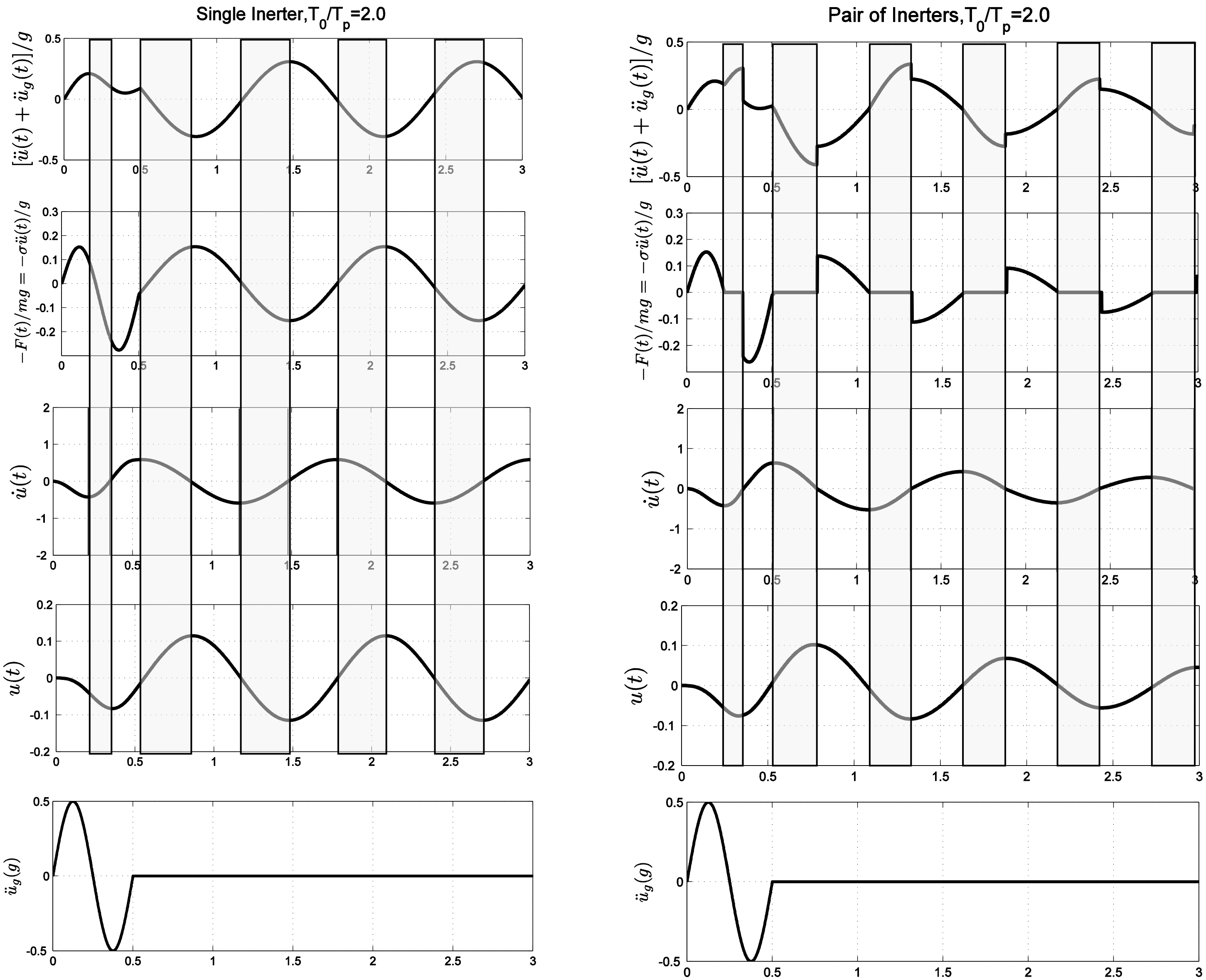

Fig. 4. Response of an inerto-elastic oscillator with an infinite stiff chevron frame. Left: Single inerter which may induce deformations; Right: Pair of inerters that can resist only the motion as described by equations (27) and (28). The force from the inerter only opposes the motion.

One challenge with the proposed concept is that the rotating flywheels should only resist the motion of the structure without inducing any deformations. This is feasible if the pinion of the first gearwheel that is engaged to the rack is unable to drive the rack and only the motion of the translating rack can drive the pinion-gearwheel. This is similar to the motion of a bicycle where the cyclist can drive the wheel through the pedals; yet, when the bicycle is rolling the pedals may remain idle. Without loss of generality, let assume that upon initiation of motion the structure moves to the left, therefore the front gearwheel rotates counterclockwise and the force on the mass from the gearwheel is to the right (positive). As the mass keeps moving to the left it will slow down and at the instant where the gearwheel will tend to drive he mass due to its angular momentum the force transmission need to become idle. With the proposed arrangement, upon the structure has reached its first maximum displacement and the motion reverses to the right ($\dot{u}(t) < 0$); the front gearwheel keeps rotating freely counterclockwise without inducing any force to the structure. When the structure starts moving to the right ($\dot{u}(t) > 0$) a second, parallel rotational inertia system (the back flywheels) is needed to oppose the motion, and during the course of this motion the first gearwheel of the back system that is engaged to the rack rotates clockwise. The sequential engagement of the two parallel rotational inertial systems that can only resist the motion is expressed mathematically:

$$\frac{F_1(t)}{m} = \sigma \ddot{u}(t) \qquad \text{when } \operatorname{sgn}\left[\frac{\ddot{u}(t)}{\dot{u}(t)}\right] > 0 \tag{25a}$$

and

$$\frac{F_1(t)}{m} = 0 \qquad \text{when } \operatorname{sgn}\left[\frac{\ddot{u}(t)}{\dot{u}(t)}\right] < 0 \tag{25b}$$

Accordingly, for the two parallel rotational inertia systems that only resist the motion of the structure, the equation of motion (15) is modified to

$$(1+\delta\sigma)\ddot{u}(t) + {\omega_0}^2 u(t) = -\ddot{u}_g(t) \tag{26}$$

in which

$$\delta = \begin{cases} 1, & when \ \operatorname{sgn}\left[\frac{\ddot{u}(t)}{\dot{u}(t)}\right] > 0 \\ 0, & when \ \operatorname{sgn}\left[\frac{\ddot{u}(t)}{\dot{u}(t)}\right] < 0 \end{cases} \tag{27}$$

Clearly, with the two parallel front and back rotational inertia systems the flywheels only resist the motion of the structure and do not induce any energy. Nevertheless, during the time-period where one of the flywheel systems is rotating idle its rotation needs to decelerate appreciably so that when it is again engaged into motion, to be capable to resist the motion through its rotational inertia. One possibility for decelerating the flywheels when rotating idle is to append to their axis an induction generator. With this arrangement, part of the earthquake induced energy will be converted into electricity that may be very much needed at that time.

Figure 4 (right) plots the same response quantities as these presented on Figure 4(left); however now, the rotating flywheels only resist the motion of the structure (when the flywheels rotate idle the transmitting force is zero and in this way throughout the response history the force from the flywheels and the velocity have always opposite signs). In this case the response of the SDOF system described with equations (26) and (27) is decaying with time since part of the seismic induced energy has been harvested through the rotation of the flywheels.

RESPONSE SPECTRA OF A MASS WITH A SPRING AND INERTER IN PARALLEL (“INDEFINITELY” STIFF CHEVRON FRAME)

The seismic response of the undamped SDOF structure with supplemental rotational inertia as described by equations (15) or (26) and (27) is compared with the seismic response of the linear damped oscillator (Clough and Penzien 1975; Chopra 2000; Symans et al. 2008)

$$\ddot{u}(t) + 2\xi_d \omega_0 \dot{u}(t) + \omega_0{}^2 u(t) = -\ddot{u}_g(t) \tag{28}$$

The values of the suppression coefficient, σ, appearing in equation (15) and the values of the damping ratio, ξ_d, appearing in equation (28) control the reduction of the response of the two systems; yet, they are also responsible for the force that is transferred to the chevron frame. Accordingly, together with the response spectra associated with the two oscillators described by equation (15) or (27) and (28) we present the peak value of the force transferred to the chevron frame, $F_1(t)$, from equations (24) or (25) and $F_d(t) = 2\xi_d m \omega_0 \dot{u}(t)$, in equation (28).

In an effort to illustrate some of the advantages and challenges when suppressing vibrations with supplemental rotational inertia we first present response spectra to pulse excitations (Veletsos et al. 1965; Bertero et al. 1978; Hall et al. 1965; Alavi and Krawinkler 2001; Mavroeidis and Papageorgiou 2003; Vassiliou and Makris 2011; among others).

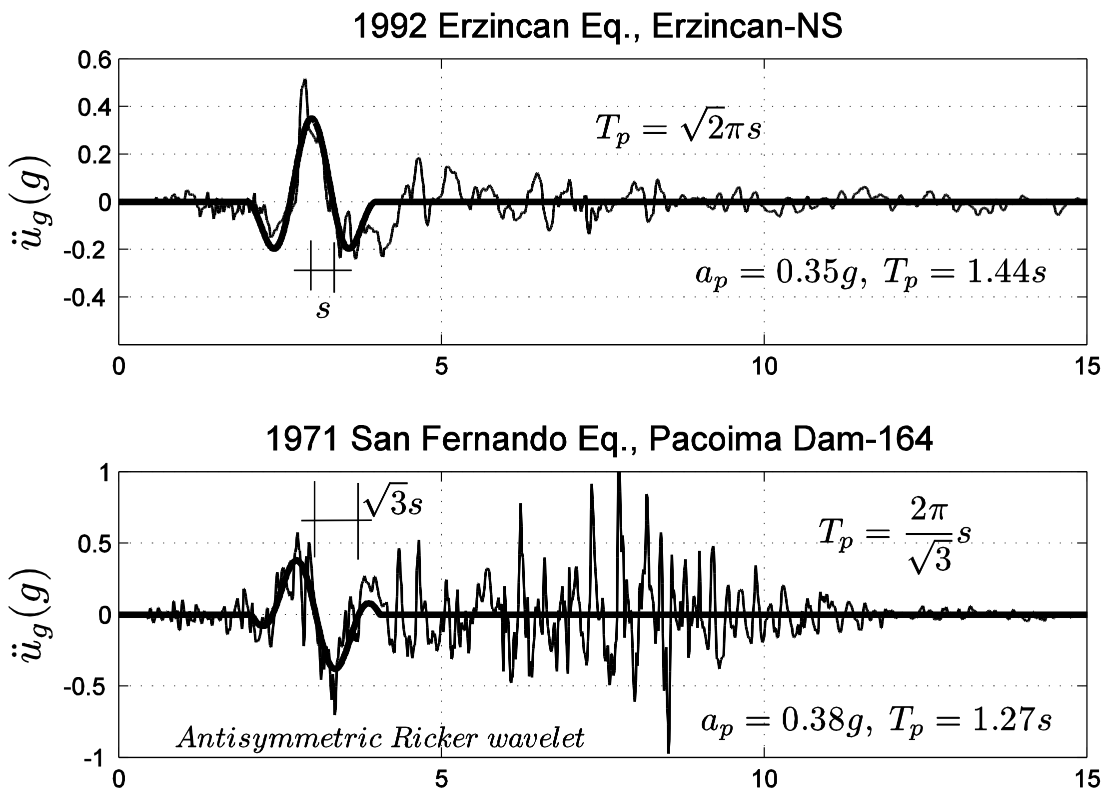

Fig. 5. Top: Nort-South component of the acceleration time history recorded during the 1992 Erzincan, Turkey earthquake together with a symmetric Ricker wavelet. Bottom: fault-normal component of the acceleration time-history recorded during the 1971 San Fernando earthquake, together with an antisymmetric Ricker wavelet.

As an example, the heavy dark line in Figure 5(top) that approximates the long-period acceleration pulse of the NS component of the 1992 Erzincan, Turkey, record is a scaled expression of the second derivative of the Gaussian distribution, $e^{-t^2/2}$, known in the seismological literature as the symmetric Ricker wavelet (Ricker 1943; Ricker 1944; see also Makris and Vassiliou 2013; Garini et al. 2014)

$$\ddot{u}_g(t) = a_p\left(1-\frac{2\pi^2 t^2}{T_p{}^2}\right)e^{-\frac{1}{2}\frac{2\pi^2 t^2}{T_p{}^2}} \qquad (29)$$

The value of the $T_p = \frac{2\pi}{\omega_p}$ is the period that maximizes the Fourier spectrum of the symmetric Ricker wavelet; therefore, $T_p = \sqrt{2}\pi s$, where s is the time from the peak pulse acceleration to the first zero crossing that follows, a_p is the acceleration amplitude of the pulse. Similarly, the heavy dark line in Figure 5(bottom), which approximates the long-period acceleration pulse of the Pacoima Dam motion recorded during the 1971 San Fernando, California, earthquake is a scaled expression of the third derivative of the Gaussian distribution , $e^{-t^2/2}$,

$$\ddot{u}_g(t) = a_p\left(\frac{2\pi^2 t^2}{T_p{}^2} - 3\right) t e^{-\frac{1}{2}\frac{2\pi^2 t^2}{T_p{}^2}} \tag{30}$$

Figure 6 plots total acceleration, relative to the ground displacement and transferred force spectra (with a sufficiently stiff chevron frame) of the SDOF system described with equations (15) or (26) and (27). For the frame with supplemental rotational inertia described by equation (15) or (26) (solid lines) values of $\sigma = 0.5$ and $\sigma = 1.0$ have been used; whereas, for the linearly damped oscillator described with equation (28) (dashed lines) values of $\xi_d = 0.1, 0.2$ and 0.3 have been used.

The first observation is that supplemental rotational inertia is effective in suppressing appreciably the peak displacement response for moderately long to long -period structures (say $T_0 / T_p > 1.5$). Spectral accelerations are suppressed within the range of moderately long periods (say $1.5s < T_0 / T_p < 3.0s$). For instance, for $T_0 / T_p = 2$ and $\sigma = 1$ both spectral accelerations and spectral displacement are appreciably lower than the corresponding spectra of a heavily damped, linear oscillator with $\xi = 30\%$. However, the corresponding forces transferred to the chevron frame are appreciably higher and in practical applications the chevron frame may experience some non-negligible deformations.

When comparing the left plots in Figure 6 which are for the single inerter described with equation (15) (that may induce displacements into the structure) with the right plots in Figure 6 which are for a pair of inerters described with equations (26) and (27) (that can only resist the motion of the structure) we make the following observation. For the case where a very stiff chevron frame is used; when a pair of inerters is employed, spectral displacement are lower for most of the spectrum; while, the forces transferred to the chevron frame are smaller only up to values of $T_0 / T_p = 2$. In this frequency range the spectral acceleration from the single inerter system are slightly lower.

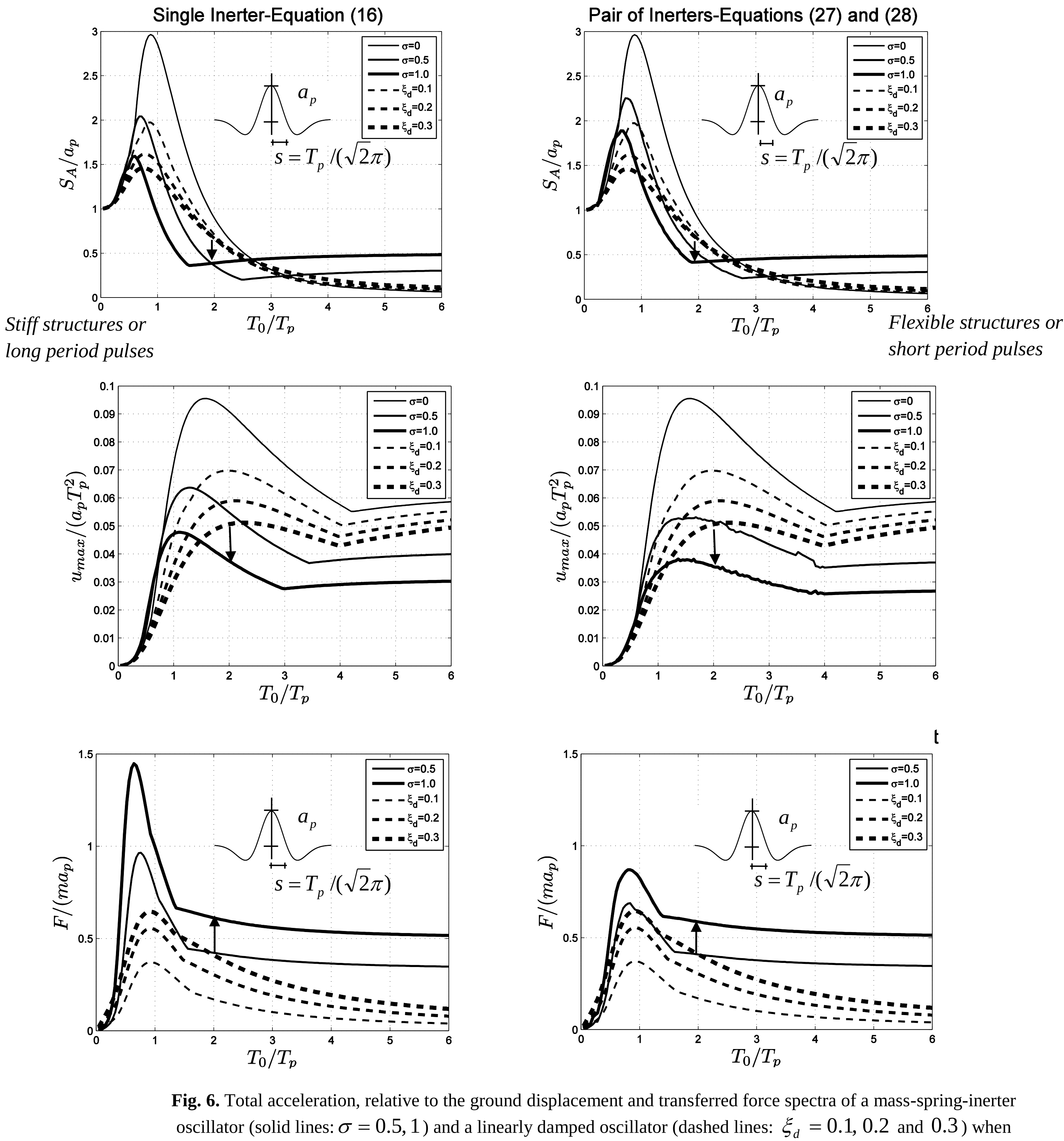

Fig. 6. Total acceleration, relative to the ground displacement and transferred force spectra of a mass-spring-inerter oscillator (solid lines: $\sigma = 0.5, 1$) and a linearly damped oscillator (dashed lines: $\xi_d = 0.1, 0.2$ and 0.3) when subjected to a symmetric Ricker pulse. Left: Single inerter which may drive occasionally the structure; Right: Pair of inerters which can only resist the motion of the structure.

RESPONSE SPECTRA WITH A CHEVRON FRAME WITH FINITE STIFFNESS AND DAMPING

We consider now the case where the support of the rotational inertia system (chevron frame) as shown in Figures 1 and 2 has a finite stiffness, k_f. In the case of bridges this support may be the stiff end abutments of the bridge, as shown in Figure 7, which when pushed against the backfill soil may mobilize appreciable damping, c_f. The proposed seismic protection strategy with supplemental rotational inertia with a rack-pinion-flywheel system at each end-abutment may be attractive for bridges which are flexible in the longitudinal direction; yet, the motion of the deck is restrained along the transverse direction at the end abutments (Makris et al. 2010). This restriction is nearly imperative in railway bridges in order to avoid misalignment of the rails at the deck-abutment joints during transverse shaking; while, it is also common in highway bridges (Kampas and Makris 2012).

Due to its finite stiffness as the rack engages with the pinion, the support of the rotational inertia systems (chevron frame) deforms by the displacement, $u_f(t)$; therefore, the displacement of the mass of the SDOF structure is

$$u(t) = u_f(t) + \rho_1\theta_1(t) \tag{31}$$

and upon differentiating two times equation (31) gives

$$\ddot{u}_f(t) = \ddot{u}(t) - \rho_1\ddot{\theta}_1(t) \tag{32}$$

The lateral displacement of the chevron frame, $\ddot{u}_f(t)$, is related to the internal force, $F_1(t)$, via the constitutive law:

$$F_1(t) = k_f u_f(t) + c_f \dot{u}_f(t) \tag{33}$$

which upon differentiating once gives:

$$\ddot{u}_f(t) = \frac{1}{c_f}\dot{F}_1(t) - \frac{k_f}{c_f}\dot{u}_f(t) \tag{34}$$

At the same time, the internal force, $F_1(t)$, that acts on the pinion of the gearwheel is given by

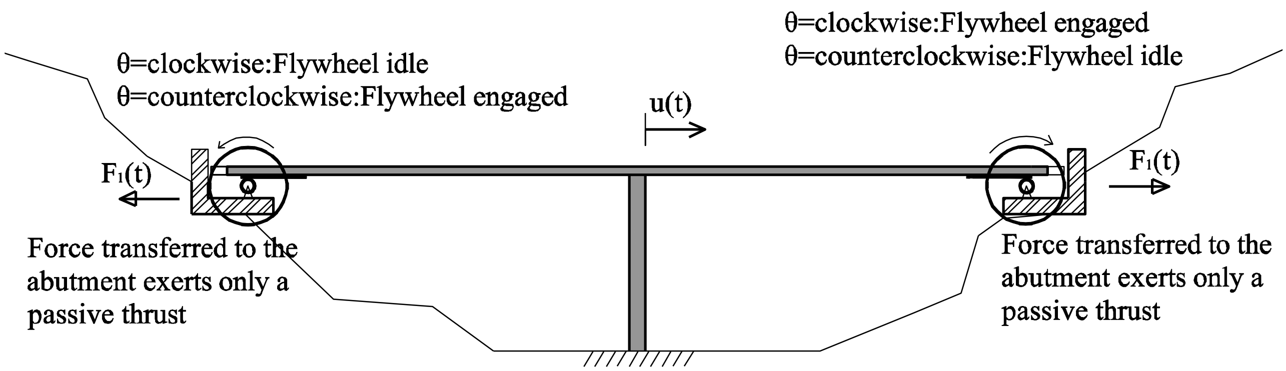

Fig. 7. Seismic protection of a bridge along the longitudinal direction with a rack-pinion-flywheel system that exerts only passive thrust on each end-abutment.

$$F_1(t) = \sigma \rho_1 m \ddot{\theta}_1(t) = M_R \rho_1 \ddot{\theta}(t) \tag{35}$$

where $\sigma m = M_R$ is the "rotational mass" of the inerter. By equating the right hand sides of the compatibility equation (32) and the constitutive equation (34) together with the help of (35) one obtains

$$\frac{1}{\sigma}\frac{F_1(t)}{m} + \frac{1}{c_f}\dot{F}_1(t) - \frac{k_f}{c_f}\dot{u}_f(t) = \ddot{u}(t) \tag{36}$$

In order to eliminate the internal variable, $\dot{u}_f(t)$, in the left-hand-side of equation (36) we differentiate once more and replace the term $\ddot{u}_f(t)$ with equation (32),

$$\frac{1}{\sigma}\frac{\dot{F}_1(t)}{m} + \frac{1}{c_f}\ddot{F}_1(t) + \frac{1}{\sigma}\frac{k_f}{c_f}\frac{F_1(t)}{m} = \frac{k_f}{c_f}\ddot{u}(t) + \dddot{u}(t) \tag{37}$$

By introducing the relaxation time of the chevron frame, $\lambda_f = \frac{c_f}{k_f} = \frac{\xi_f}{\pi}T_f$, where $T_f = 2\pi\sqrt{\frac{m}{k_f}}$, is the period of the system when "locked" to the chevron frame; equation (37) becomes

$$\frac{1}{\sigma}\left(\frac{F_1(t)}{m} + \lambda_f \frac{\dot{F}_1(t)}{m} + \tau^2 \frac{\ddot{F}_1(t)}{m}\right) = \ddot{u}(t) + \lambda_f \dddot{u}(t) \tag{38}$$

in which the parameter

$$\tau = \sqrt{\frac{\sigma m}{k_f}} = \sqrt{\frac{M_R}{k_f}} \tag{39}$$

is defined as the reatardation time of the system.

Equation (38) indicates that in the case where a SDOF structure is protected with a supplemental rotational inertia system that is supported on a chevron frame with finite stiffness, k_f, and damping, $c_f = 2\xi_f m\omega_f$ $(\omega_f = \sqrt{k_f / m})$, the internal force, $F_1(t)$, satisfies the differential equation (38) rather than the algebraic equation (24) that is for an infinite stiff frame. In the special case where the damping of the chevron frame is neglected, $c_f = 0$; therefore, $\lambda_f = 0$, equation (38) reduces to

$$\frac{F_1(t)}{m} + \tau^2 \frac{\ddot{F}_1(t)}{m} = \sigma\ddot{u}(t) \tag{40}$$

In this special case, there is no need to involve the third derivative of the ground displacement in the time-domain analysis. In order to obtain practical values of the retardation time, τ, let assume that the chevron frame is N times stiffer than the SDOF structure; that is, $k_f = Nk = Nm\omega_0^{\;2}$. Accordingly, the normalized retardation time to the undamped natural frequency of the structure $T_0 = 2\pi / \omega_0$ is given by

$$\frac{\tau}{T_0} = \frac{1}{2\pi}\sqrt{\frac{\sigma}{N}} \tag{41}$$

For a chevron frame that is 20 to 100 times stiffer than the SDOF structure and for values of the suppression coefficient $\sigma = 0.5$ and 1, the range of practical values for τ / T_0 is $0.01 \le \tau / T_0 \le 0.04$.

When $k_f = Nk$, the "locked" period of the system $T_f = 2\pi\sqrt{\frac{m}{Nk}} = \frac{1}{\sqrt{N}}T_0$. Accordingly, the normalized relaxation time of the system to the undamped natural frequency of the structure, $T_0 = 2\pi / \omega_0$ is given by

$$\frac{\lambda_f}{T_0} = \frac{\xi_f}{\pi} \frac{1}{\sqrt{N}} \tag{42}$$

Equation (42) indicates that the range of practical values for λ_f / T_0 is $0.01 < \lambda_f / T_0 < 0.001$.

In this analysis we are also adding a small amount of viscous damping in the SDOF structure (say $\xi = 2\%$). Accordingly, the equation of motion of the damped SDOF structure with supplemental rotational inertia shown in Figure 3 (right) is

$$\ddot{u}(t) + 2\xi\omega_0\dot{u}(t) + \omega_0{}^2 u(t) + \frac{F_1(t)}{m} = -\ddot{u}_g(t) \tag{43}$$

in which the internal force $F_1(t)/m$ is given by equation (38).

The response of the system with supplemental rotational inertia shown in Figure 3(right) is compared with the response of a heavily damped SDOF structure where the seismic protection is achieved with supplemental viscous damping with damping constant, $C_d = 2\xi_d m\omega_0$. In this case, the chevron frame also deforms and it can be shown by following a similar analysis (Constantinou et al. 1998) that the damping force, F_d, that develops in the supplemental damper satisfies a Maxwell equation

$$\frac{F_d(t)}{m} + \lambda \frac{\dot{F}_d(t)}{m} = 2\xi_d\omega_0\dot{u}(t) \tag{44}$$

where $\lambda = C_d / k_f$, is known as the relaxation time of the system. For a chevron frame that is N times stiffer than the SDOF structure, $k_f = Nk$, the normalized relaxation time to the undamped natural frequency of the structure, $T_0 = 2\pi / \omega_0$, is given by

$$\frac{\lambda}{T_0} = \frac{1}{\pi} \frac{\xi_d}{N} \tag{45}$$

For a chevron frame that is 20 to 100 times stiffer than the SDOF structure and for values of $0.1 \le \xi_d \le 0.3$ the range of practical values of λ / T_0 is $0.0005 \le \lambda / T_0 \le 0.005$.

When the chevron frame that supports the supplemental damper with damping constant, $C_d = 2\xi_d m\omega_0$ is as strong as the chevron frame that supports the supplemental inerter with inertial mass, $M_R = \sigma m$, the relaxation time, λ, appearing in equation (45) is related to the retardation time, τ, appearing in equation (41) via the equation

$$\lambda = \frac{2\xi_d \omega_0}{\sigma} \tau^2 \tag{46}$$

The solution of the system of differential equations given by (43) and (38) is computed numerically via a state-space formulation. The state vector of the system is

$$\{y(t)\} = \begin{Bmatrix} y_1(t) \\ y_2(t) \\ y_3(t) \\ y_4(t) \end{Bmatrix} = \begin{Bmatrix} u(t) \\ \dot{u}(t) \\ F_1(t)/m \\ \dot{F}_1(t)/m \end{Bmatrix} \tag{47}$$

and the time-derivative of the state vector, $\{\dot{y}(t)\}$, is expressed in terms of the state variables as

$$\{\dot{y}(t)\} = \begin{Bmatrix} y_2(t) \\ -\ddot{u}_g(t) - 2\xi\omega_0 y_2(t) - \omega_0{}^2 y_1(t) - y_3(t) \\ y_4(t) \\ \dfrac{\sigma\lambda_f}{\tau}\{-\dddot{u}_g(t) - 2\xi\omega_0[-\ddot{u}_g(t) - 2\xi\omega_0 y_2(t) - \omega_0{}^2 y_1(t) - y_3(t)] - \omega_0{}^2 y_2(t) - y_4(t)\} \\ \qquad + \dfrac{\sigma}{\tau^2}[-\ddot{u}_g(t) - 2\xi\omega_0 y_2(t) - \omega_0{}^2 y_1(t) - y_3(t)] - \dfrac{1}{\tau^2} y_3(t) - \dfrac{\lambda_f}{\tau^2} y_4(t) \end{Bmatrix} \tag{48}$$

The numerical integration of equations (48) is performed with standard ODE solvers available in MATLAB (2002).

Alternatively, given that equations (38) and (43) are linear differential equations, the response history of the SDOF-system can be computed with the Fourier transform,

$$u(t) = \frac{1}{2\pi}\int_{-\infty}^{+\infty} \mathcal{U}(\omega) e^{i\omega t} d\omega \tag{49}$$

where

$$\mathcal{U}(\omega) = -\frac{1-\omega^2\tau^2 + i\omega\lambda_f}{(1-\omega^2\tau^2 + i\omega\lambda_f)(\omega_0{}^2 - \omega^2 + 2i\xi\omega_0\omega) - \sigma\omega^2(1+i\omega\lambda_f)} \ddot{\mathcal{U}}_g(\omega) \tag{50}$$

When a single rotational inertia system is used, the frequency domain solution offered by equations (49) and (50) is attractive since it does not involve the differentiation of the ground acceleration. The agreement of the time-domain solution expressed with equations (38) and (43) and the frequency domain solution given by equations (49) and (50) has been confirmed during the course of this study.

The response of the SDOF structure with supplemental damping with constant $C_d = 2\xi_d m\omega_0$ is also computed with equation (49); where now

$$\mathcal{U}(\omega) = -\frac{1}{\omega_0{}^2 - \omega^2 + 2i\xi\omega_0\omega + \dfrac{2i\xi_d\omega_0\omega}{1+i\omega\lambda}} \ddot{\mathcal{U}}_g(\omega) \tag{51}$$

When the two parallel rotational inertia system are employed which can only resist the motion of the structure without inducing any deformations (the pinion of the gearwheel that is engaged to the rack is unable to drive the rack and only the motion of the translating rack can drive the pinion), the term $F_1(t)/m$ appearing in equation (43) is given by equation (38) when $\mathrm{sgn}\left[\frac{\ddot{u}(t)}{\dot{u}(t)}\right] > 0$ and by

$$\frac{F_1(t)}{m} = 0 \qquad \text{when } \mathrm{sgn}\left[\frac{\ddot{u}(t)}{\dot{u}(t)}\right] < 0 \tag{52}$$

In this case the equation of motion of our SDOF structure becomes piece-wise linear and only a time-domain solution is feasible. The state vector of the system is given by equation (47) when $\mathrm{sgn}[\ddot{u}(t)/\dot{u}(t)] > 0$ and by

$$\{y(t)\} = \begin{Bmatrix} y_1(t) \\ y_2(t) \end{Bmatrix} = \begin{Bmatrix} u(t) \\ \dot{u}(t) \end{Bmatrix} \qquad \text{when } \operatorname{sgn}\left[\frac{\ddot{u}(t)}{\dot{u}(t)}\right] < 0 \tag{53}$$

Figure 8 plots total acceleration, relative to the ground displacement and transferred force spectra of the SDOF system described with equations (48) or with equations (48) and (53) for $\sigma = 0.5$ and $\sigma = 1.0$, $\lambda_f / T_0 = 0.01$ and three different values of the dimensionless retardation time $\tau / T_0 = 0.01, 0.02$ and 0.04 when the SDOF system is excited by a symmetric Ricker wavelet described with equation (29). The time derivative of the ground acceleration appearing in the fourth component of the time-derivative of the state vector given by equation (48) is offered by equation (30) –that is the antisymmetric Ricker pulse. For the linearly damped oscillator where the damping force from the supplemental dampers that resist on the chevron frame is given by equation (44), values of $\xi_d = 0.1$ and 0.3 have been used.

The first observation (as in the case of the infinite stiff chevron frame) is that the supplemental rotational inertia is effective in suppressing appreciably the peak displacement response for moderately long to long-period structures (say $T_0 / T_p > 1.5$). Spectral accelerations are suppressed within the range of moderately long periods (say $1.5 < T_0 / T_p < 3.0$); nevertheless, this is true only for small values of the retardation time ($\tau / T_0 < 0.02$ –stiff chevron frames). When the chevron frame is less stiff spectral accelerations increase appreciably for longer-period structures. When comparing the left plots in Figure 8 which are for a single rotational inertia system described continuously with equation (47) or with equations (49) and (50) (that may induce displacements into the structure) with the right plots in Figure 8 which are for a pair (front and back) of rotational inertia systems described by equations (48) and (53) (that can only resist the motion of the structure) we make the following observation. The pair of rotational inertia systems control the spectral accelerations and forces transferred for large values of T_0 / T_p; however, the response is sensitive to the retardation time, τ (finite stiffness of the system). It is concluded that the strategy of suppressing vibrations with supplemental rotational inertia is attractive when the support of the rotational inertia system is stiff ($\tau / T_0 < 0.02$).

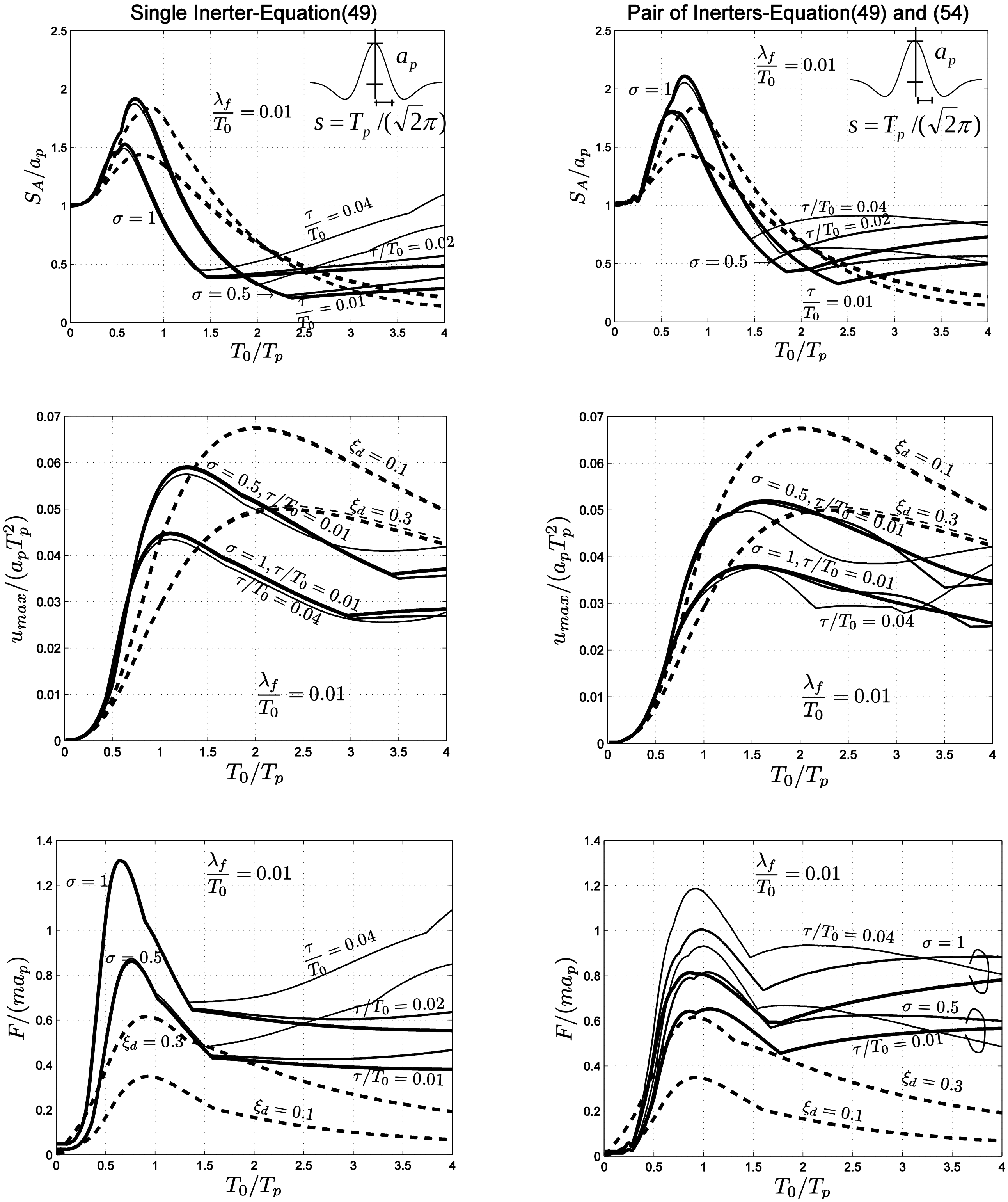

Fig. 8. Total acceleration, relative to the ground displacement and transferred force spectra of a mass-spring-inerter oscillator (solid lines: $\sigma = 0.5, 1$ and three values of retardation times: $\tau / T_0 = 0.01,\ 0.02$ and 0.04) and a linearly damped oscillator (dashed lines: $\xi_d = 0.1$ and 0.3) when subjected to a symmetric Ricker pulse. Left: Single inerter which may drive occasionally the structure; Right: Pair of inerters which can only resist the motion of the structure.

CONCLUSIONS

In this paper we investigated the potential advantages of the alternative strategy of suppressing ground-induced vibrations with supplemental rotational inertia. The proposed concept employs a rack-pinion-flywheel system that its resisting force is proportional to the relative acceleration between the vibrating mass and the support of the flywheels. The paper shows that the seismic protection of structures with supplemental rotational inertia has the unique advantage of suppressing the spectral displacements of long period structures –a function that is not efficiently achieved even with large values of supplemental damping. Furthermore, the proposed strategy can accommodate large relative displacements without suffering from the issues of viscous heating and potential leaking that challenge the implementation of fluid dampers. At the same time, the paper shows that the forces transferred to the support of the rotational inertia system are appreciable and that the use of stiff supports is recommended ($\tau / T_0 < 0.02$).

This paper examines the dynamic response of a SDOF structure when two parallel rotational inertia systems are installed so that they can only resist the motion of the structure without inducing any deformation. This can be achieved if the pinion of each of the gearwheels of the two parallel rotational inertia systems that is engaged to the rack is unable to drive the rack and only the motion of the translating rack can drive the pinion-gearwheel. This arrangement reduces further the spectral displacements; whereas, the results for the forces transferred to the support of the gearwheels are mixed.

Finally, the proposed concept where reduction of vibrations is achieved with supplemental rotational inertia so that the resisting force is proportional to the relative acceleration introduces the subject of inerto-visco-elasticity.

REFERENCES

1. Alavi B, Krawinkler H. (2001). *Effects of Near-Source Ground Motions on Frame-Structures*. John A. Blume Earthquake Engineering Center Rept. **138**, Stanford University.
2. Bertero VV, Mahin SA, Herrera RA. (1978). “A seismic design implications of near-fault San Fernando earthquake records.” *Earthq. Eng. Struct. Dyn.*, 6, 31-42.
3. Black CJ, Makris N, Aiken ID. (2004). “Component Testing Seismic Evaluation and Characterization of Buckling Restrained Braces.” *Journal of Structural Engineering, ASCE,* 130(6), 880-894.

4. Chopra, A. (2000). *Dynamics of Structures: Theory and Applications to Earthquake Engineering*. Prentice-Hall International Series in Civil Engineering and Engineering Mechanics.
5. Clough RW, Penzien J. (1975). *Dynamics of Structures*. McGraw-Hill.
6. Constantinou MC, Soong TT, Dargush GF. (1998). "Passive Energy Dissipation Systems for Structural Design and Retrofit." *MCEER-98-MN01*, Buffalo, NY.
7. Direct-Lift Drawbridges without Cables. (1913). *Engineering News*, 69(23), 1168-1170.
8. Garini E, Makris N, Gazetas G. (2014). "Elastic and Inelastic Systems under Near-Fault Seismic Shaking: Acceleration Records versus Optimally-Fitted Wavelets." *Bulletin of Earthquake Engineering*, DOI 10.1007/s10518-014-9631-z.
9. Giaralis A, Taflanidis AA. (2015). "Reliability-based Design of Tuned Mass-Dampers-Inerter (TMDI) Equipped Multi-storey Frame Buildings under Seismic Excitation." *12th International Conference on Applications of Statistics and Probability in Civil Engineering, ICASP12*, Vancouver, Canada.
10. Hahin, C. (1998). "Investigation of Rack and Pinion Alignment of the Street Movable Bridge in Joliet. Illinois." *Physical Research Report* No.129, Illinois Department of Transportation, Springfield, Illinois.
11. Hall JF, Heaton TH, Halling MW, Wald DJ. (1965). "Near-source ground motion and its effects on flexible buildings." *Earthq. Spect*, 11, 569-605.
12. Housner GW. (1963). "The behavior of inverted pendulum structures during earthquakes" *Bull. Seism. Soc. Am.* 53(2), 404–417.
13. Kampas G, Makris N. (2012). "Transverse versus Longitudinal Eigenperiods of Multispan Seismically Isolated Bridges." *J. Struct. Eng.*, 138(2), 193–204.
14. Kelly JM. (1997). *Earthquake-resistant Design with Rubber*. Springer: London.
15. Kirkpatrick P. (1927). "Seismic measurements by the overthrow of columns." *Bull. Seismol. Soc. Am.*, 17, 95-109.
16. Makris N. (2015). "A Half-Century of Rocking Isolation." *Earthquakes and Structures*, 7**(**2), DOI: 10.12989/eas.2014.7.6.000.
17. Makris N. (2014). "The Role of the Rotational Inertia on the Seismic Resistance of Free-Standing Rocking Columns and Articulated Frames." *Bull. Seismol. Soc. Am.*, 104(5), 2226-2239.
18. Makris N, Chang SP. (2000). "Response of Damped Oscillators to Cyclical Pulses." *Journal of Engineering Mechanics ASCE* , 126(2), 123-131.

19. Makris, N, Chang SP. (2000). “Effect of Viscous, Viscoplastic and Friction Damping on the Response of Seismic Isolated Structures.” *Earthquake Engineering and Structural Dynamics*, 29, 85-107.
20. Makris N, Kampas G, Angelopoulou D. (2010). “The eigenvalues of isolated bridges with transverse restraints at the end abutments.” *Earthquake Engineering & Structural Dynamics*, 39(8), 869-886.
21. Makris N., Kampas G. (2016). “Size Versus Slenderness: Two Competing Parameters in the Seismic Stability of Free-Standing Rocking Columns.”, *Bull. Seism. Soc. Am*, doi:10.1785/0120150138.
22. Marian L, Giaralis A. (2013). “Optimal design of inerter devices combined with TMDs for vibration control of buildings exposed to stochastic seismic excitations.” *11th International Conference on Structural Safety and Reliability*, paper #137, 1025-1032.
23. Marian L, Giaralis A. (2014). “Optimal design of a novel tuned mass-damper-inerter (TMDI) passive vibration control configuration for stochastically support-excited structural systems.” *Prob Eng Mech*, 38, 156-164.
24. MATLAB. (2002). *High-performance Language Software for Technical Computation*. The MathWorks, Inc: Natick, MA.
25. Mavroeidis GP, Papageorgiou AS. (2003). “A mathematical representation of near-fault ground motions.” *Bull. Seismol. Soc. Am.*, 93, 1099-1131.
26. Movable Bridge Engineering. Maintenance, (2014). *Repair and Rehabilitation Series PTA-M5*, Illinois Department of Transportation, Springfield, Illinois.
27. Naeim, F, and Kelly, JM. (1999). *Design of Seismic Isolated Structures*. New York: Wiley Publications.
28. Papageorgiou C, Smith MC. (2005). “Laboratory experimental testing of inerters.” *IEEE Conference on Decision and Control*, 44, 3351-3356.
29. Patton WJ. (1980). *Mechanical Power Transmission*, Prentice-Hall.
30. PTDA. (2014). *Power Transmission Handbook*. Power Transmission Distributors Association, Chicago IL, USA.
31. Ricker N. (1943). “Further developments in the wavelet theory of seismogram structure”, *Bull. Seism. Soc. Am*, 33, 197–228.
32. Ricker N. (1944). “Wavelet functions and their polynomials”, *Geophysics* 9, 314–323.
33. Smith MC. (2002). “Synthesis of Mechanical Networks: The Inerter.” *IEEE Transactions on Automatic Control*, 47(10), 1648-1662.

34. Symans MD, Charney FA, Whittaker AS, Constantinou MC, Kircher CA, Johnson MW, McNamara RJ. (2008). "Energy Dissipation Systems for Seismic Applications: Current Practice and Recent Developments", *Journal of Stuctural Engineering*, 134(1), 3-21.

35. Vassiliou MF, Makris N. (2011). "Estimating Time Scales and Length Scales in Earthquake Acceleration Records with Wavelet Analysis." *Bulletin of the Seismological Society of America*, 101, 596-618.

36. Veletsos AS, Newmark NM, Chelepati CV. (1965). "Deformation spectra for elastic and elastoplastic systems subjected to ground shock and earthquake motions." *Proceedings of the 3rd World Conference on Earthquake Engineering*, Wellington, New Zealand, II, 663–682.

FIGURE CAPTIONS

Fig. 1. Left: A single-degree-of-freedom structure with mass, m, and stiffness, k, with supplemental rotational inertia from a flywheel with radius, R, supported on a chevron frame with stiffness, k_f, that is much larger than k; Right: Free-body diagram of the vibrating mass, m, when engaged to the pinion of the flywheel shown below.

Fig. 2. More than one flywheels in series that amplify the effect of supplemental rotational inertia.

Fig. 3. Left: Schematic of a mass-spring-inerter single-degree-of-freedom system: the inerto-elastic oscillator; Right: The inerto-visco-elastic oscillator.

Fig. 4. Response of an inerto-elastic oscillator with an infinite stiff chevron frame. Left: Single inerter which may induce deformations; Right: Pair of inerters that can resist only the motion as described by equations (27) and (28). The force from the inerter only opposes the motion.

Fig. 5. Top: Nort-South component of the acceleration time history recorded during the 1992 Erzincan, Turkey earthquake together with a symmetric Ricker wavelet. Bottom: fault-normal component of the acceleration time-history recorded during the 1971 San Fernando earthquake, together with an antisymmetric Ricker wavelet.

Fig. 6. Total acceleration, relative to the ground displacement and transferred force spectra of a mass-spring-inerter oscillator (solid lines: $\sigma = 0.5, 1$) and a linearly damped oscillator (dashed lines: $\xi_d = 0.1, 0.2$ and 0.3) when subjected to a symmetric Ricker pulse. Left: Single inerter which may drive occasionally the structure; Right: Pair of inerters which can only resist the motion of the structure.

Fig. 7. Seismic protection of a bridge along the longitudinal direction with a rack-pinion-flywheel system that exerts only passive thrust on each end-abutment.

Fig. 8. Total acceleration, relative to the ground displacement and transferred force spectra of a mass-spring-inerter oscillator (solid lines: $\sigma = 0.5, 1$ and three values of retardation times: $\tau / T_0 = 0.01, 0.02$ and 0.04) and a linearly damped oscillator (dashed lines: $\xi_d = 0.1$ and 0.3) when subjected to a symmetric Ricker pulse. Left: Single inerter which may drive occasionally the structure; Right: Pair of inerters which can only resist the motion of the structure.